Ultrasound in Med. & Biol., Vol. 47, No. 3, pp. 438–445, 2021

0301-5629/$ - see front matter

https://doi.org/10.1016/j.ultrasmedbio.2020.11.009

● *Original Contribution*

CLINICAL FEASIBILITY OF QUANTITATIVE ULTRASOUND IMAGING FOR SUSPECTED HEPATIC STEATOSIS: INTRA- AND INTER-EXAMINER RELIABILITY AND CORRELATION WITH CONTROLLED ATTENUATION PARAMETER

Sun Kyung Jeon,*,† Jeong Min Lee,*,†,‡ and Ijin Joo*,†

* Department of Radiology, Seoul National University Hospital, Seoul, Korea; † Seoul National University College of Medicine, Seoul, Korea; and ‡ Institute of Radiation Medicine, Seoul National University Medical Research Center, Seoul, Korea

(*Received* 11 *April* 2020; *revised* 13 *October* 2020; *in final from* 9 *November* 2020)

Abstract—This study was aimed at investigating the clinical feasibility of quantitative ultrasound (QUS) imaging in the evaluation of suspected hepatic steatosis through assessment of the reliability of measurements and its correlation with the controlled attenuation parameter (CAP). This retrospective study included 117 patients who underwent liver B-mode ultrasound (US) with QUS imaging with a clinical US machine (RS85, Samsung Medison, Seoul, Korea) and CAP measurements between December 2019 and March 2020. For QUS examination, tissue attenuation imaging (TAI) and tissue scatter-distribution imaging (TSI) parameters were obtained. Intra- and inter-examiner reliability were assessed using intra-class correlation coefficients (ICCs), and QUS imaging parameters were correlated with CAP measurements using Spearman's correlation analysis. TAI and TSI revealed excellent intra- and inter-examiner reliability with ICCs of 0.994 and 0.975 and 0.991 and 0.947, respectively. Both TAI and TSI were significantly positively correlated with CAP values. QUS imaging provided good intra-and inter-observer reliability and correlated well with CAP in assessing suspected hepatic steatosis. (E-mail: jmsh@snu.ac.kr) **© 2020 World Federation for Ultrasound in Medicine & Biology. All rights reserved.**

Key Words: **Ultrasonography, Quantitative imaging, Liver, Steatosis, Reproducibility, Reliability, Attenuation.**

INTRODUCTION

Hepatic steatosis is a major histologic feature of non-alcoholic fatty liver disease (NAFLD) and is associated with other chronic liver diseases, including chronic viral hepatitis or alcoholic liver disease (Ma et al. 2009). Although percutaneous liver biopsy remains the gold standard for hepatic steatosis, it has associated complications, sampling errors and inter-reader variability (Bravo et al. 2001; Wildman-Tobriner et al. 2018). Hence, biopsy is performed only when strictly necessary, and non-invasive diagnostic tools for hepatic steatosis are urgently required (Rinella 2015; Zhou et al. 2019).

Non-invasive tools that are developed and used for assessing hepatic steatosis include various imaging tools, including ultrasound (US), the controlled attenuation parameter (CAP), magnetic resonance (MR) spectroscopy and the MR-proton density fat fraction (PDFF) (Wildman-Tobriner et al. 2018). Among these, US is commonly the first-line imaging test in patients with suspected NAFLD (McCarthy and Stroud 1989); it provides good sensitivity and specificity for moderate to severe steatosis (sensitivity = 84.8% and specificity = 93.6%) (Hernaez et al. 2011). However, US also has the following limitations: insufficient objectivity, inter-observer variability, system variability and limited diagnostic performance in detecting mild steatosis <20% (sensitivity = 65.0% and specificity = 81.0%) or steatosis in individuals with morbid obesity (Dasarathy et al. 2009; Hernaez et al. 2011; Chalasani et al. 2018).

In recent years, quantitative ultrasound (QUS), such as the ultrasonic attenuation coefficient and backscatter coefficient, derived from the raw radiofrequency echo data, has been considered as a non-invasive tool in objective assessment of hepatic steatosis (Lin et al. 2015; Paige et al. 2017; Han et al. 2018; Tada et al. 2019). In our recent study, two QUS parameters (tissue scatter-distribution imaging [TSI] and tissue attenuation imaging [TAI]) of the liver parenchyma were derived from radiofrequency echo data and exhibited good diagnostic performance for predicting hepatic steatosis in patients with

Address correspondence to: Jeong Min Lee, Department of Radiology, Seoul National University Hospital and Seoul National University College of Medicine, 101 Daehangno, Jongno-gu, Seoul, 03080, Korea. E-mail: jmsh@snu.ac.kr

chronic liver disease (Jeon et al. 2020) Currently, these are approved for clinical use in a commercially available US system (RS85, Samsung Medison, Seoul, Korea). TSI is measured by averaging the Nakagami shape pixels in the region of interest (ROI). Therefore, the TSI map represents the regional concentration and distribution of US scatterers (Tsui et al. 2015; Wan et al. 2015). TAI is obtained by calculating the slope of the US center frequency downshifts with depth. It estimates the attenuation in the ROI (Kim and Varghese 2007). However, little is known about the clinical feasibility and reproducibility of TAI and TSI in a clinically available US system (RS85 A) for hepatic steatosis.

This study was aimed at investigating the clinical feasibility of QUS imaging in evaluating hepatic steatosis by assessing its reliability and correlation with CAP.

METHODS

Study population

This retrospective study was approved by the institutional review board, and written informed consent was waived. We included 117 patients who underwent both B-mode US examination, including QUS (TAI and TSI), and transient elastography (TE) with CAP on the same day between December 2019 and March 2020. The indications for US examinations were as follows: suspected NAFLD (n = 57), suspected chronic liver disease or liver cirrhosis for surveillance of hepatocellular carcinoma (n = 30), workup for the evaluation of hepatic metastasis (n = 11) and health checkup (n = 19).

Acquisition of B-mode and quantitative US

Participants were requested to fast for at least 6 h before B-mode US. One board-certified radiologist (J.M. L., with 27 y of experience in abdominal imaging) performed conventional gray-scale US with QUS imaging using a clinical US system (RS85 A) with a convex probe (CA1-7 A). Routine B-mode liver US images were obtained during a breath-hold using subcostal and intercostal planes and stored for evaluation of the visual grade of hepatic steatosis.

Thereafter, two sessions of QUS examinations were performed on the same day in each patient, and each session acquired five consecutive measurements of the attenuation coefficient (AC) at TAI and scatter-distribution coefficient (SC) at TSI. First, during breath-hold, B-mode images were acquired from the right lobe of the liver in the intercostal plane near the level of the hepatic hilum. Subsequently, with the selection of a function key for TAI or TSI, a 2 × 3-cm ROI with a color-coded map was generated and overlaid on the B-mode image. Avoiding areas with large vessels, focal fat sparing or deposition and reverberation artifacts or shadowing, the ROI box was placed in a relatively homogeneous region in the right lobe of the liver at least 2 cm below the liver capsule (Yoo et al. 2019). Areas with significant errors in the calculation of parameters, such as vascular structures, were automatically excluded from the maps. The AC at TAI and SC at TSI of the ROI were automatically calculated, and their R^2 values were provided (Fig. 1). According to the vendors' recommendation, the radiologist attempted to obtain color maps with an R^2 value $\geq$0.6. The mean values of AC at TAI and SC at TSI in each session were used for analysis. Additionally, the mean values of TAI and TSI between the two sessions were used to calculate intra-observer reproducibility. Furthermore, as one session of QUS measurement was performed by another radiologist (S.K.J., with 6 y of experience in liver imaging) in the initial period of using QUS, those data were used to evaluate inter-observer reliability.

Visual scoring of hepatic steatosis on B-mode US

All stored B-mode US images were independently reviewed by two radiologists (J.M.L. and S.K.J.). If any interpretations revealed discrepancies between the radiologists, they re-evaluated the images together and reached a consensus. Hepatic steatosis was diagnosed based on known US findings, including increased parenchymal echogenicity, hepatorenal echo contrast, impaired visualization of the diaphragm line and intrahepatic portal vein wall and deep attenuation of the liver parenchymal echo (Ballestri et al. 2012). Additionally, the severity of hepatic steatosis was qualitatively scored on a 4-point scale using the Hamaguchi scoring system (Hamaguchi et al. 2007), with scores of 0, 1, 2 and 3 indicating no, mild, moderate and severe steatosis, respectively.

Transient elastography with CAP

On TE (Fibroscan, Echosens, Paris, France), CAP (in dB/m) and liver stiffness (in kPa) were measured using an M probe based on the manufacturer's recommendations (Zhang et al. 2020). For each participant, the median of 10 valid measurements was considered representative of CAP and liver stiffness measurement (LSM), respectively (Chon et al. 2014). Both CAP and LSM were considered reliable if the 10 valid measurements had an interquartile range/median $<$0.3 (Castera et al. 2008; Semmler et al. 2020). CAP values were used to determine hepatic steatosis grades based on the cutoff values suggested in previous study (Chon et al. 2014): 0−250 dB/m for S0 (no steatosis), $>$250 dB/m for S1 (mild steatosis), $>$299 dB/m for S2 (moderate steatosis) and $>$327 dB/m for S3 (severe steatosis). LSM values on TE were used to determine hepatic fibrosis grades by applying the cutoff values suggested in a previous study (Castéra et al. 2005): 0−7.1 kPa for

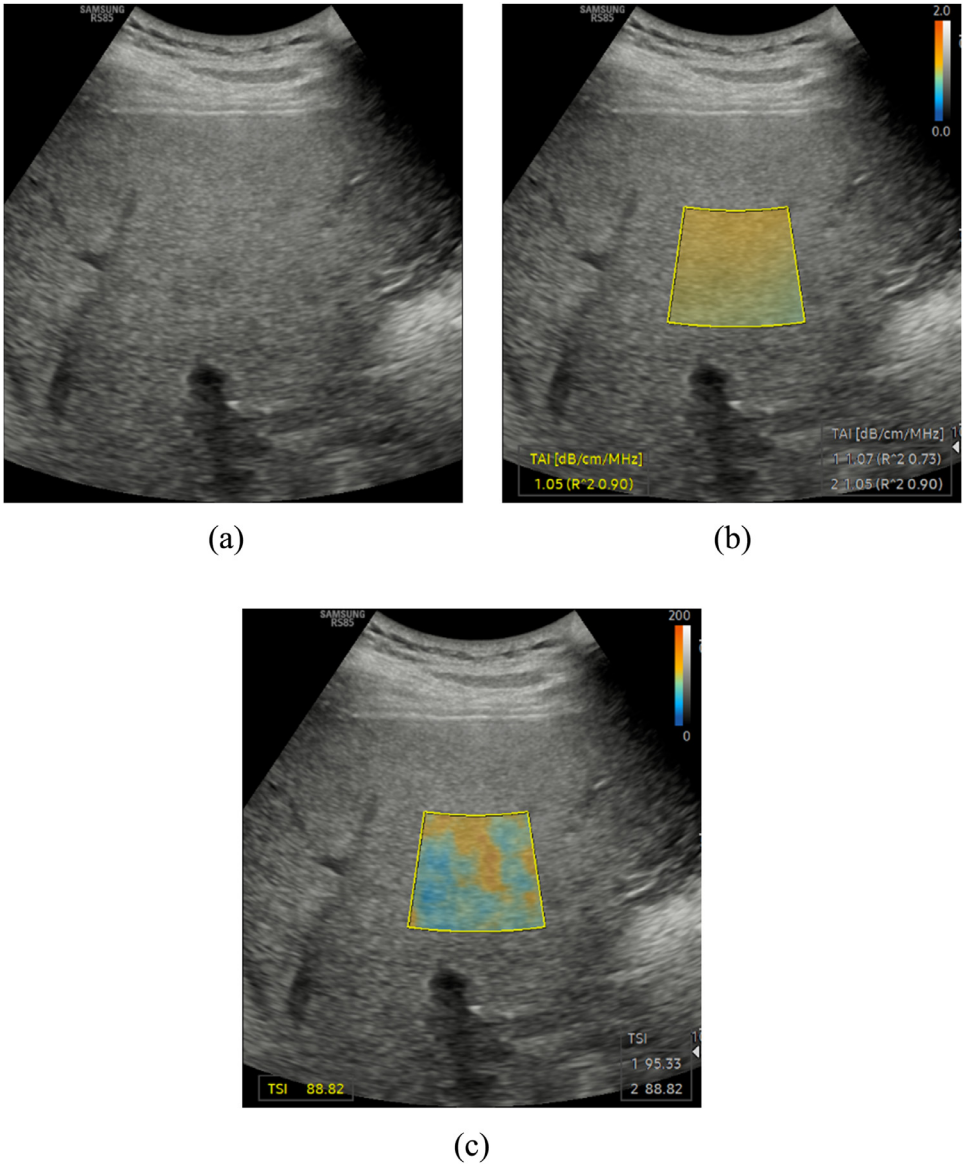

Fig. 1. Example of quantitative ultrasound (QUS) imaging including tissue attenuation imaging (TAI) and tissue scatter-distribution imaging (TSI). After acquisition of an adequate sonic window on the B-mode ultrasound image (a), QUS examinations including TAI (b) and TSI (c) were performed. The level of attenuation (a) and Nakagami parameters (b) are color-coded and displayed in the region of interest of the TAI map (a) and TSI map (b), respectively. The ultrasound system automatically displays the attenuation coefficient (AC) at TAI parameter with the coefficient of determination (R^2 value) (b) and scatter-distribution coefficient (SC) at TSI (c), respectively.

≤F1 (no or mild fibrosis), >7.1 kPa for ≥F2 (significant fibrosis), >9.5 kPa for ≤F3 (severe fibrosis), and >12.5 kPa for F4 (cirrhosis).

Statistical analyses

Independent sample *t*-tests and χ^2-tests were used for comparison of continuous variables and categorical variables between patients with reliable and unreliable CAP values, respectively. Intra- and inter-observer reliability was assessed using the intra-class correlation coefficients (ICCs) and interpreted as follows: ≥0.90, excellent; ≥0.75 to <0.90, good; ≥0.50 to <0.75, moderate; and <0.50, poor reliability (Koo and Li 2016). The coefficient of variation (CV) was also calculated to provide an additional estimation of intra- and inter-observer reliability, with a small CV value indicating more reliable measurements (Bland and Altman 1986). Subgroup analysis of intra-observer reliability according to sex (male/female), body mass index (BMI) (<25 kg/m^2 or ≥25 kg/m^2),

skin-to-capsule distance (<20 mm or ≥20 mm), visual hepatic steatosis grade (<S2 or ≥S2), hepatic steatosis grade based on CAP value (<S2 or ≥S2) and hepatic fibrosis grade (<F2 or ≥F2) was performed using ICC estimates with 95% confidence intervals and their CVs. The F-test was used to compare CVs.

Correlations between SC at TSI or AC at TAI and visual grades of hepatic steatosis or CAP values were assessed using Spearman's rank correlation analysis. Spearman's correlation coefficient (ρ) was interpreted as follows: $|\rho| > 0.5$, strong correlation; $|\rho| = 0.3-0.5$, moderate correlation; and $|\rho| < 0.3$, weak correlation (Kobus et al. 2016). As the Kolmogorov–Smirnov test revealed that AC at TAI and SC at TSI did not follow a normal distribution, US parameters of different steatosis grades were compared with the Kruskal–Wallis test followed by Dunn's *post hoc* test. In Dunn's *post hoc* test, a Bonferroni-adjusted p value <0.017 (0.05/3) was considered to indicate statistical significance as three pairwise comparisons between adjacent grades were performed.

Statistical analyses were performed using MedCalc 16.4.1 (MedCalc Software, Ostend, Belgium) and the Statistical Package for the Social Sciences, Version 25.0 (IBM Corp. Armonk, NY, USA). A p value < 0.05 was considered to indicate statistical significance, except for the aforementioned pairwise comparison tests.

RESULTS

Study population

A total of 117 patients (52 men and 65 women; age, mean ± standard deviation [SD]: 54.8 ± 14.0 y; and BMI, mean ± SD: 24.6 ± 3.7 kg/m^2) were included. Patient characteristics are summarized in Table 1. As 97 patients underwent two examinations by a single operator, while 20 patients underwent examinations by two operators, data from 97 and 20 patients were used to evaluate intra- and inter-observer reliability, respectively. Of the 117 patients, only 97 patients had reliable CAP and liver stiffness (LS) measurements. Therefore, the CAP- or LS-related analysis was performed in 97 patients. Of the 97 patients with reliable CAP values, patients were classified as having S0, S1, S2 and S3 based on CAP values in 34, 26, 17 and 20, respectively. Based on LSM values on TE, 12 patients (12.4%) were categorized as having significant hepatic fibrosis (≥F2). Patients with unreliable CAP values (n = 20) had significantly lower BMI (22.6 ± 3.0 kg/m^2 vs. 24.9 ± 3.7 kg/m^2, $p = 0.011$) and smaller skin-to-liver distance (16.0 ± 2.8 mm vs. 18.8 ± 3.7 mm, $p = 0.001$). There were no significant differences in age and sex between patients with and without reliable CAP values ($p > 0.05$).

Table 1. Patient characteristics (N = 117)

Characteristic	No. of patients
Age (y), mean ± SD (range)	54.8 ± 14.0 (18–86)*
Sex (male:female)	52 (44.4%):65 (55.6%)
Body mass index (kg/m^2)	24.6 ± 3.7 (16.9–34.9)
Skin-liver capsule distance (mm)	18.3 ± 3.8 (10.7–28.9)
Aspartate aminotransferase (IU/L)	32.9 ± 46.7 (14–101)
Alanine aminotransferase (IU/L)	40.8 ± 61.8 (6–131)
Hepatic fibrosis grade	
<F2 (without significant hepatic fibrosis, ≤7.1 kPa on TE)	85 (87.6%)
≥F2 (with significant hepatic fibrosis, >7.1 kPa on TE)	12 (12.4%%)
Visual hepatic steatosis grade	
S0	37 (31.6%)
S1	24 (20.5%)
S2	42 (35.9%)
S3	11 (9.4%)
Hepatic steatosis grades based on CAP (N = 97)*	
S0 (≤250 dB/m on CAP)	34 (35.1%)
S1 (>250 to ≤299 dB/m on CAP)	26 (26.8%)
S2 (>299 to ≤327 dB/m on CAP)	17 (17.5%)
S3 (>327 dB/m on CAP)	20 (20.6%)

Values are expressed as the mean ± standard deviation (range) or number (%) unless otherwise specified.
TE = transient elastography; CAP = controlled attenuation parameter.
* CAP-related analysis was performed only in patients with reliable CAP measurement (N = 97).

Intra- and inter-observer reliability in TSI and tissue attenuation imaging

The intra-observer reliabilities of TAI and TSI of the liver parenchyma were both excellent, with ICCs of 0.994 and 0.975 and CVs of 2.2% and 3.1%. The inter-observer reliability of TAI and TSI was also excellent, with ICCs of 0.991 and 0.947 and CVs of 2.7% and 3.1% (Table 2). Moreover, CVs were not associated with sex, BMI, skin-to-capsule distance, hepatic fibrosis grade or hepatic steatosis grade ($p > 0.05$; Table 3).

Table 2. Intra-observer and inter-observer reliability of TAI and TSI

Parameter	AC at TAI	SC at TSI
Intra-observer reliability (N = 97)		
Intra-class correlation coefficient	0.994 (0.991–0.996)	0.975 (0.963–0.984)
Coefficient of variation (%)	2.2 (1.8–2.5)	3.1 (2.6–3.6)
Inter-observer reliability (N = 20)		
Intra-class correlation coefficient	0.991 (0.977–0.996)	0.947 (0.867–0.979)
Coefficient of variation (%)	2.7 (1.8–3.6)	3.1 (2.1–4.1)

Values in parentheses are 95% confidence intervals. AC= attenuation coefficient, TAI = tissue attenuation imaging, SC = scatter-distribution coefficient, TSI = tissue scatter-distribution imaging.

Table 3. Subgroup analysis of intra-observer reliability of TAI and TSI (n = 97)

Variable	ACat TAI			SC at TSI		
	ICC	CV (%)	*p* Value	ICC	CV (%)	*p* Value
Sex			0.526			0.991
Male (n = 43)	0.995 (0.991−0.997)	2.0 (1.6−2.5)		0.969 (0.943−0.983)	3.0 (2.4−3.7)	
Female (n = 54)	0.993 (0.988−0.996)	2.2 (1.8−2.6)		0.979 (0.964−0.988)	3.0 (2.5−3.7)	
Body mass index (kg/m^2)			0.217			0.649
<25 (n = 59)	0.992 (0.987−0.995)	2.3 (1.8−2.7)		0.978 (0.962−0.987)	3.0 (2.4−3.5)	
≥25 (n = 38)	0.995 (0.990−0.997)	1.9 (1.4−2.3)		0.947 (0.898−0.972)	3.2 (2.4−3.9)	
Skin-to-capsule distance (mm)			0.144			0.724
<20 (n = 70)	0.992 (0.987−0.995)	2.2 (1.9−2.6)		0.976 (0.961−0.985)	3.1 (2.6−3.6)	
≥20 (n = 27)	0.995 (0.990−0.998)	1.7 (1.3−2.2)		0.942 (0.873−0.974)	2.9 (2.1−3.7)	
Visual hepatic steatosis grade			0.096			0.379
<S2 (n = 56)	0.972 (0.953−0.984)	2.4 (1.9−2.8)		0.959 (0.930−0.976)	3.2 (2.6−3.8)	
≥S2 (n = 41)	0.993 (0.987−0.996)	1.9 (1.3−2.5)		0.920 (0.849−0.957)	2.8 (2.2−3.5)	
Hepatic steatosis grade based on CAP (N = 78)			0.052			0.067
<S2 (n = 53)	0.978 (0.962−0.987)	2.6 (1.4−3.4)		0.951 (0.916−0.972)	4.1 (3.1−4.9)	
≥S2 (n = 25)	0.995 (0.988−0.998)	1.8 (0.9−2.3)		0.913 (0.804−0.962)	2.9 (2.0−3.5)	
Hepatic fibrosis grade (N = 78)			0.747			0.831
<F2 (without significant fibrosis) (n = 67)	0.994 (0.990−0.996)	2.0 (1.4−2.5)		0.963 (0.940−0.978)	3.8 (3.0−4.4)	
≥F2 (with significant fibrosis) (n = 11)	0.997 (0.988−0.999)	2.1 (0.4−2.9)		0.972 (0.894−0.992)	3.5 (0.0−5.4)	

Values in parentheses are 95% confidence intervals. *p* values are derived from comparison of coefficients of variation of subgroups.
AC= attenuation coefficient; TAI = tissue attenuation imaging; SC = scatter-distribution coefficient; TSI = tissue scatter-distribution imaging; ICC = intraclass correlation coefficient; CV = coefficient of variation.

Correlation of QUS parameters with visual grades of hepatic steatosis scores and CAP values

Tissue attenuation imaging and tissue scatter-distribution imaging parameters based on visual hepatic steatosis grades or hepatic steatosis grades based on CAP values are given in Table 4 and Figure 2. Both TAI and TSI parameters significantly correlated with visual grades of hepatic steatosis ($\rho = 0.883$ and 0.788, 95% confidence intervals = 0.836−0.918 and 0.708−0.848, respectively, $p < 0.001$). Additionally, both TAI and TSI parameters significantly correlated with CAP values ($\rho = 0.799$ and 0.679, and 95% confidence intervals = 0.713−0.861 and 0.555−0.774, respectively, $p < 0.001$).

Table 4. US parameters according to hepatic steatosis grades

Hepatic steatosis grade	AC at TAI (dB/cm/MHz)	SC at TSI
Visual steatosis grade (N = 117)		
S0 (n = 37)	0.66 ± 0.05	69.4 ± 7.2
S1 (n = 24)	0.75 ± 0.07	77.4 ± 7.4
S2 (n = 42)	0.88 ± 0.09	87.8 ± 5.9
S3 (n = 11)	1.11 ± 0.13	90.3 ± 4.5
Steatosis grade based on CAP value (N = 97)*		
S0 (n = 34)	0.69 ± 0.07	72.2 ± 8.2
S1 (n = 26)	0.81 ± 0.07	83.6 ± 8.1
S2 (n = 17)	0.85 ± 0.12	88.1 ± 7.0
S3 (n = 20)	1.03 ± 0.13	89.4 ± 3.9

Values are expressed as the mean ± standard deviation.
CAP = controlled attenuation parameter; AC= attenuation coefficient; TAI = tissue attenuation imaging; SC = scatter-distribution coefficient; TSI = tissue scatter-distribution imaging.
* CAP-related analysis was performed only in patients with a reliable CAP measurement (N = 97).

By use of visual hepatic steatosis grades, both AC at TAI and SC at TSI significantly differed according to steatosis grade ($p < 0.001$). In comparisons of each steatosis grade, both AC at TAI and SC at TSI significantly differed between S0 and S1 or between S1 and S2 (p values <0.001). On the contrary, only AC at TAI significantly differed between S2 and S3 ($p < 0.001$), while SC at TSI did not exhibit a significant difference ($p = 0.199$).

When hepatic steatosis grades based on CAP values were used, both AC at TAI and SC at TSI significantly differed according to steatosis grade ($p < 0.001$). When S0 and S1 were compared, both AC at TAI and SC at TSI significantly differed ($p < 0.001$), while AC at TAI and SC at TSI did not significantly differ between S1 and S2 ($p > 0.999$ and 0.434, respectively) or between S2 and S3 ($p = 0.053$ and $p > 0.999$, respectively).

DISCUSSION

This study found that AC at TSI and SC at TSI measurements have excellent intra- and inter-observer reliability. Of note, intra-observer reliability of AC at TAI and SC at TSI was not associated with BMI, skin-to-capsule distance or hepatic fibrosis grade. Additionally, both AC at TAI and SC at TSI correlated well with visual hepatic steatosis grade and CAP value. These

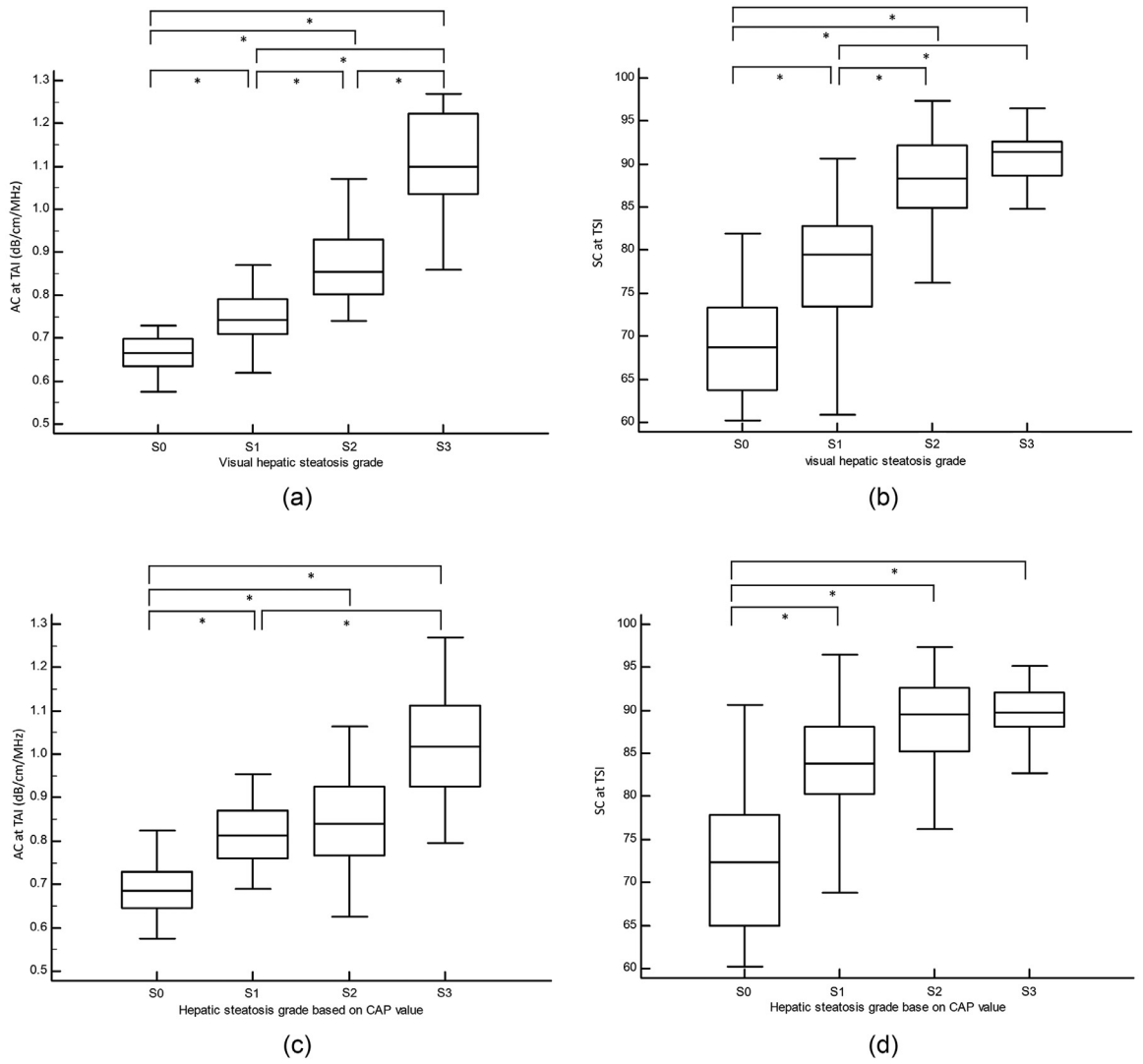

Fig. 2. Box-and-whisker plots of the attenuation coefficient (AC) at tissue attenuation imaging (TAI) (a,c) and scattter-dstribution coefficient (SC) at tissue scatter-distribution imaging (TSI) (b,d) based on visual hepatic steatosis grade (a,b) and hepatic steatosis grade based on the controlled attenuation parameter values (c,d). Boxes represent the median and 25th and 75th percentiles, and whiskers represent the minimum and maximum values. Asterisks indicate significant differences between steatosis grades using the Kruskal−Wallis test with Dunn' s *post hoc* test.

results support the clinical applicability of TSI and TAI for assessment of suspected hepatic steatosis, and QUS parameters can be easily added as an adjunctive objective tool to evaluate suspected hepatic steatosis.

In this study, AC at TAI significantly positively correlated with visual steatosis grade and CAP value, indicating attenuation of the US beam increased as steatosis grade increased. Previous studies on attenuation imaging also found a similar positive correlation between attenuation coefficient and hepatic steatosis grade (Fujiwara et al. 2018; Bae et al. 2019). SC at TSI also significantly positively correlated with visual steatosis grade and CAP value. When the concentration of fat droplets (the acoustic scatterers) increases in a homogeneous medium such as liver parenchyma, US backscattered statistics shift from a pre-Rayleigh to a Rayleigh distribution, which increases TSI (Wan et al. 2015). These results were consistent with a previous study on US backscatter parameters in NAFLD (Han et al. 2019).

Although both AC at TAI and SC at TSI significantly correlated with both visual steatosis grade and CAP value, the distributions of the two parameters according to steatosis grade were relatively different. In this study, AC at TAI values significantly differed across all visual steatosis grades (*i.e.,* significant differences between S0 and S1, S1 and S2, and S2 and S3). Consistent with previous studies of attenuation imaging, AC at TAI is considered beneficial in detecting

and quantifying hepatic steatosis. In contrast, SC at TSI did not significantly differ between S2 and S3 steatosis, with significant differences only between S0 and S1 or S1 and S2. Considering the results of our study, although SC at TSI can be used to detect mild to moderate hepatic steatosis, there are difficulties in accurate fat quantification or differentiation between moderate and severe steatosis. However, as early detection of hepatic steatosis at a mild degree is important as it enables timely management of hepatic steatosis, which may prevent further progression of disease (Chalasani et al. 2018), our results suggest the potential application of SC at TSI as a screening method for hepatic steatosis; however, the diagnostic accuracy and optimal cutoff values should be further validated. Additionally, the wide range in values of SC at TSI at S0 grade (no steatosis) could be another drawback in the application of screening methods for hepatic steatosis, and further validation studies are required.

Of note, in our study, we found that both TAI and TSI had high intra- and inter-observer reliability. Furthermore, intra-observer reliability was not associated with BMI, skin-to-capsule distance, hepatic fibrosis grade or hepatic steatosis grade. Considering these results, we believe that both TAI and TSI can play important roles as screening tests in patients with hepatic steatosis with wide applicability.

Our study has several limitations. First, as a retrospective study, our study population was heterogeneous, with suspected NAFLD or various chronic liver diseases. Considering that the steatosis pattern could vary depending on the etiology of liver disease, further studies evaluating the performance of both TAI and TSI with respect to the etiology are required. Also, the reproducibility of QUS techniques with respect to the various etiologies would also be warranted. In addition, as our study did not confirm the hepatic steatosis by histopathology, the reliability of QUS techniques should be validated through a further study by using MRI-PDFF or histopathologic results as the reference standard. Second, we correlated AC at TAI and SC at TSI with visual hepatic steatosis grade and CAP value, rather than histopathology results or MR-PDFF. Although visual steatosis grade is a commonly used grading tool for hepatic steatosis in routine clinical practice and CAP is a well-validated tool for hepatic fat quantification, they have several drawbacks, including limitations in detecting mild hepatic steatosis and influence from several covariates such as BMI (Castera et al. 2019). Further studies with histologic results are required to validate our study results and evaluate the diagnostic performance of QUS for the evaluation of hepatic steatosis.

In conclusion, QUS imaging provided good intra- and inter-observer reliability and correlated well with CAP in assessing suspected hepatic steatosis.

Acknowledgments—This study was supported by a grant from the Seoul National University Research Fund (03-2018-0230).

REFERENCES

Bae JS, Lee DH, Lee JY, Kim H, Yu SJ, Lee JH, Cho EJ, Lee YB, Han JK, Choi BI. Assessment of hepatic steatosis by using attenuation imaging: A quantitative, easy-to-perform ultrasound technique. Eur Radiol 2019;29:6499–6507.

Ballestri S, Lonardo A, Romagnoli D, Carulli L, Losi L, Day CP, Loria P. Ultrasonographic fatty liver indicator, a novel score which rules out NASH and is correlated with metabolic parameters in NAFLD. Liver Int 2012;32:1242–1252.

Bland JM, Altman D. Statistical methods for assessing agreement between two methods of clinical measurement. The lancet 1986;327:307–310.

Bravo AA, Sheth SG, Chopra S. Liver biopsy. N Engl J Med 2001;344:495–500.

Castéra L, Vergniol J, Foucher J, Le Bail B, Chanteloup E, Haaser M, Darriet M, Couzigou P, de Lédinghen V. Prospective comparison of transient elastography, Fibrotest, APRI, and liver biopsy for the assessment of fibrosis in chronic hepatitis C. Gastroenterology 2005;128:343–350.

Castera L, Forns X, Alberti A. Non-invasive evaluation of liver fibrosis using transient elastography. Journal of hepatology 2008;48:835–847.

Castera L, Friedrich-Rust M, Loomba R. Noninvasive assessment of liver disease in patients with nonalcoholic fatty liver disease. Gastroenterology 2019;156 1264–1281. e4.

Chalasani N, Younossi Z, Lavine JE, Charlton M, Cusi K, Rinella M, Harrison SA, Brunt EM, Sanyal AJ. The diagnosis and management of nonalcoholic fatty liver disease: Practice guidance from the American Association for the Study of Liver Diseases. Hepatology 2018;67:328–357.

Chon YE, Jung KS, Kim SU, Park JY, Park YN, Kim DY, Ahn SH, Chon CY, Lee HW, Park Y. Controlled attenuation parameter (CAP) for detection of hepatic steatosis in patients with chronic liver diseases: A prospective study of a native Korean population. Liver International 2014;34:102–109.

Dasarathy S, Dasarathy J, Khiyami A, Joseph R, Lopez R, McCullough AJ. Validity of real time ultrasound in the diagnosis of hepatic steatosis: A prospective study. J Hepatol 2009;51:1061–1067.

Fujiwara Y, Kuroda H, Abe T, Ishida K, Oguri T, Noguchi S, Sugai T, Kamiyama N, Takikawa Y. The B-mode image-Guided ultrasound attenuation parameter accurately detects hepatic steatosis in chronic liver disease. Ultrasound Med Biol 2018;44:2223–2232.

Hamaguchi M, Kojima T, Itoh Y, Harano Y, Fujii K, Nakajima T, Kato T, Takeda N, Okuda J, Ida K, Kawahito Y, Yoshikawa T, Okanoue T. The severity of ultrasonographic findings in nonalcoholic fatty liver disease reflects the metabolic syndrome and visceral fat accumulation. Am J Gastroenterol 2007;102:2708–2715.

Han A, Andre MP, Deiranieh L, Housman E, Erdman JW, Jr., Loomba R, Sirlin CB, O'Brien WD, Jr. Repeatability and reproducibility of the ultrasonic attenuation coefficient and backscatter coefficient measured in the right lobe of the liver in adults with known or suspected nonalcoholic fatty liver disease. J Ultrasound Med 2018;37:1913–1927.

Han A, Boehringer AS, Zhang YN, Montes V, Andre MP, Erdman JW, Loomba R, Sirlin CB, O'Brien WD. Improved assessment of hepatic steatosis in humans using multi-parametric quantitative ultrasound. 2019 IEEE International Ultrasonics Symposium (IUS). : IEEE; 2019. p. 1819–1822.

Hernaez R, Lazo M, Bonekamp S, Kamel I, Brancati FL, Guallar E, Clark JM. Diagnostic accuracy and reliability of ultrasonography for the detection of fatty liver: A meta-analysis. Hepatology 2011;54:1082–1090.

Jeon SK, Joo I, Kim SY, Jang JK, Park J, Park HS, Lee ES, Lee JM. Quantitative ultrasound radiofrequency data analysis for the assessment of hepatic steatosis using the controlled attenuation parameter as a reference standard [e-pub ahead of print]. Ultrasonography 2020. doi: 10.14366/usg.20042 Accessed 2020 July 4 [Epub].

Kim H, Varghese T. Attenuation estimation using spectral cross-correlation. IEEE Trans Ultrason Ferroelectr Freq Control 2007;54:510–519.

Kobus T, van der Laak JA, Maas MC, Hambrock T, Bruggink CC, Hulsbergen-van de Kaa CA, Scheenen TW, Heerschap A. Contribution of histopathologic tissue composition to quantitative MR spectroscopy and diffusion-weighted imaging of the prostate. Radiology 2016;278:801–811.

Koo TK, Li MY. A guideline of selecting and reporting intraclass correlation coefficients for reliability research. Journal of chiropractic medicine 2016;15:155–163.

Lin SC, Heba E, Wolfson T, Ang B, Gamst A, Han A, Erdman JW, Jr., O'Brien WD, Jr., Andre MP, Sirlin CB, Loomba R. Noninvasive diagnosis of nonalcoholic fatty liver disease and quantification of liver fat using a new quantitative ultrasound technique. Clin Gastroenterol Hepatol 2015;13 1337−1345 e6.

Ma X, Holalkere NS, Mino-Kenudson M, Hahn PF, Sahani DV. Imaging-based quantification of hepatic fat: Methods and clinical applications. Radiographics 2009;29:1253–1277.

McCarthy MP, Stroud RM. Conformational states of the nicotinic acetylcholine receptor from Torpedo californica induced by the binding of agonists, antagonists, and local anesthetics. Equilibrium measurements using tritium-hydrogen exchange. Biochemistry 1989;28:40–48.

Paige JS, Bernstein GS, Heba E, Costa EAC, Fereirra M, Wolfson T, Gamst AC, Valasek MA, Lin GY, Han A, Erdman JW, Jr., O'Brien WD, Jr., Andre MP, Loomba R, Sirlin CB. A pilot comparative study of quantitative ultrasound, conventional ultrasound, and MRI for predicting histology-determined steatosis grade in adult nonalcoholic fatty liver disease. AJR Am J Roentgenol 2017;208:W168–w77.

Rinella ME. Nonalcoholic fatty liver disease: A systematic review. Jama 2015;313:2263–2273.

Semmler G, Wöran K, Scheiner B, Unger LW, Paternostro R, Stift J, Schwabl P, Bucsics T, Bauer D, Simbrunner B, Stättermayer AF, Pinter M, Trauner M, Reiberger T, Mandorfer M. Novel reliability criteria for controlled attenuation parameter assessments for non-invasive evaluation of hepatic steatosis. United European Gastroenterol J 2020;8:321–331.

Tada T, Iijima H, Kobayashi N, Yoshida M, Nishimura T, Kumada T, Kondo R, Yano H, Kage M, Nakano C, Aoki T, Aizawa N, Ikeda N, Takashima T, Yuri Y, Ishii N, Hasegawa K, Takata R, Yoh K, Sakai Y, Nishikawa H, Iwata Y, Enomoto H, Hirota S, Fujimoto J, Nishiguchi S. Usefulness of attenuation imaging with an ultrasound scanner for the evaluation of hepatic steatosis. Ultrasound Med Biol 2019;45:2679–2687.

Tsui PH, Wan YL, Tai DI, Shu YC. Effects of estimators on ultrasound Nakagami imaging in visualizing the change in the backscattered statistics from a Rayleigh distribution to a pre-Rayleigh distribution. Ultrasound Med Biol 2015;41:2240–2251.

Wan YL, Tai DI, Ma HY, Chiang BH, Chen CK, Tsui PH. Effects of fatty infiltration in human livers on the backscattered statistics of ultrasound imaging. Proceedings of the Institution of Mechanical Engineers, Part H: Journal of Engineering in Medicine 2015;229:419–428.

Wildman-Tobriner B, Middleton MM, Moylan CA, Rossi S, Flores O, Chang ZA, Abdelmalek MF, Sirlin CB, Bashir MR. Association between magnetic resonance imaging-proton density fat fraction and liver histology features in patients with nonalcoholic fatty liver disease or nonalcoholic steatohepatitis. Gastroenterology 2018;155 1428−1435 e2.

Yoo J, Lee JM, Joo I, Lee DH, Yoon JH, Kang HJ, Ahn SJ. Reproducibility of ultrasound attenuation imaging for the noninvasive evaluation of hepatic steatosis. Ultrasonography 2019.

Zhang X, Wong GL, Wong VW. Application of transient elastography in nonalcoholic fatty liver disease. Clinical and molecular hepatology 2020;26:128–141.

Zhou JH, Cai JJ, She ZG, Li HL. Noninvasive evaluation of nonalcoholic fatty liver disease: Current evidence and practice. World J Gastroenterol 2019;25:1307–1326.